GFZ
Helmholtz-Zentrum
POTSDAM

Originally published as:

Zöller, G., Hainzl, S., Holschneider, M., Brietzke, G. B. (2011): Steady-state solutions of rupture propagation in an earthquake simulator governed by rate and state dependent friction. - European Physical Journal B, 191, 1, 105-115

DOI: 10.1140/epjst/e2010-01344-6

EPJ manuscript No.
(will be inserted by the editor)

Steady-state solutions of rupture propagation in an earthquake simulator governed by rate and state dependent friction

Gert Zöller[1,a] Sebastian Hainzl[2] Matthias Holschneider[1] and Gilbert Brietzke[2]

[1] Institute of Mathematics, Am Neuen Palais 10, 14469 Potsdam, Germany
[2] Deutsches GeoForschungsZentrum Potsdam, Telegrafenberg, 14473 Potsdam

Abstract. Earthquake simulators become increasingly important with respect to seismic hazard assessment. It is, therefore, a crucial question whether the imposed simplifications, e.g. reducing fully dynamic to quasi-dynamic rupture propagation, may lead to unrealistic results. In the present study, we focus on the role of rupture velocity v_r in an earthquake simulator governed by rate-and-state dependent friction as proposed by [8]. In particular, we investigate the range of possible values of v_r within the model. As an end-member scenario, we consider the existence of a steady-state solution of a one-dimensional rupture front propagating with v_r on an idealized two-dimensional fault of infinite dimension discretized into uniform cells. We find that, in principle, values of v_r between 0 and ∞ are possible depending on the values of slip speed $\dot{\delta}_0$ and pre-stress τ_0 ahead of the rupture front. In this view, values of $\dot{\delta}_0$ close to the slip speed during an earthquake $\dot{\delta}_{EQ}$ lead to small values of the time-to-failure and can thus generate ruptures with unrealistic high values of v_r, if the model is close to the steady-state conditions. These results are useful to provide constraints for the parameter space of a reasonable earthquake simulator.

1 Introduction

In recent decades, numerical models for simulating earthquake occurrence have been used to improve the understanding of the earthquake process and to estimate the resulting seismic hazard in the future. Different models cover a broad range between two end-member classes; first, detailed physical simulations of the dynamic rupture process [2,4] of a specific event and second, calculations of thousands of years of earthquake evolution in models with reduced complexity. The pros and cons are obvious: The first model class allows for realistic description of a particular event, but is related with high numerical effort and several poorly-constrained parameters. In contrast the latter class provides less realistic simulations; these models, however, allow for robust statistics, because a large number of events may be generated. Models of this type, generally labeled as "earthquake simulators" [3,8,11,13,17,18,20,21], become increasingly popular for seismic hazard calculations, since they overcome the problem of small data sets (earthquake catalogs), at least to some degree. The tightrope walk is now to find the most relevant mechanisms that govern the dynamics of the earthquake process and to keep the model as simple as possible, simultaneously. Less important processes may be neglected or plugged into a stochastic component [11,12,20] leading to a hybrid-model (deterministic/stochastic). We note that purely stochastic models are also widely applied; here, the empirical knowledge of

[a] e-mail: zoeller@uni-potsdam.de

the frequency-size distribution, aftershock decay and productivity is accounted for and provides constraints for Monte-Carlo simulations [13,19,12].

The central question with respect to the use of an earthquake simulator is: To what extent does a model simulate realistic earthquake histories, despite the imposed simplifications? These include mainly: first, the deformation process including continuous evolution from locked fault segments which start to nucleate and finally end up in an earthquake, is replaced by the instantaneous transitions between three discrete states (locked, nucleating, slipping); second, the dynamic Green's function is replaced by the static Green's function. This question has been addressed for many seismicity features like the Gutenberg-Richter law [10] and the Omori law [15]. In this study, we focus on a physics-based earthquake simulator firstly proposed by [8], which reduces a time-continuous to a time-discrete model based on rate-and-state dependent friction (RS friction) [6,7,9,16]. The model allows to simulate the inter- and co-seismic propagation of stress and displacement in finite time on a discrete spatial grid. This is in contrast to other models like cellular automata models [1], where co-seismic process occur instantaneously. The goal of this work is to identify regions in parameter space which are characterized by almost realistic behavior of rupture evolution in terms of rupture speed. To keep the model setup as simple as possible, we a study one-dimensional rupture front of infinite size traveling through an elastic full-space governed by RS friction and address the question, which values of the rupture speed v_r are possible.

In Section 2, we give a description of the model, including geometrical setup, the basic features of RS friction and the implementation of two model versions for a one-dimensional rupture front. In Section 3, the simulations and the results are provided. Finally the results are discussed, especially with respect to their impact for improving earthquake simulators.

2 Model

In this Section, we describe the geometrical setup of the model, the framework of RS friction, and the algorithm of the model. More details are provided in [8] and [9].

2.1 Geometrical setup

The geometry of the model is visualized in Fig. 1. It includes a vertical strike slip fault embedded in a homogeneous elastic half-space. In an idealized picture a rupture front of infinite dimension travels along the space in negative x direction. Since we impose symmetry with respect to depth (z axis), the half space becomes effectively a full-space, in this limit.

2.1.1 Rate-and-state dependent friction (RS friction)

In this work, we follow the Ruina formulation [16] of Dieterich's law [5] for the frictional resistance during the earthquake process. During slip the shear stress τ and the effective normal stress σ follow

$$\tau = \sigma \left[\mu_0 + A \ln \left(\frac{\dot{\delta}}{\dot{\delta}^*} \right) + B \ln \left(\frac{\theta}{\theta^*} \right) \right]. \tag{1}$$

Here, μ_0, σ, A, and B are constants determined from experiments, $\dot{\delta}$ is the slip speed, and $\dot{\delta}^*$ and θ^* are normalizing constants, where θ^* can be expressed by the characteristic slip distance D_c,

$$\theta^* = \frac{D_c}{\dot{\delta}^*}. \tag{2}$$

The state variable θ in Eq. (1) follows the evolution law [16]

$$\frac{d\theta}{dt} = 1 - \frac{\theta \dot{\delta}}{D_c}. \tag{3}$$

In [6] Eq. (1) and (3) are used to simulate earthquake nucleation on a fault patch with stiffness K and linear remote stressing rate $\dot{\tau}t$ $\tau(t)$,

$$\tau(t) = \tau_0 + \dot{\tau}t, \tag{4}$$

resulting in the following relation for the evolution of slip speed:

$$\dot{\delta} = \left\{ \left[\frac{1}{\dot{\delta}_0} + \frac{H\sigma}{\dot{\tau}} \right] \left[\exp\left(-\frac{\dot{\tau}t}{A\sigma} \right) \right] - \frac{H\sigma}{\dot{\tau}} \right\}^{-1}, \ \dot{\tau} \neq 0. \tag{5}$$

where $\dot{\delta}_0$ is the initial slip speed, $H = B/D_c - K/\sigma$.

2.1.2 Cellular automaton version

A space-discrete fault model may be designed by solving the equations from the previous subsection on a discrete grid with heterogeneous parameters. To reduce the computational effort and thus to allow for long simulations of earthquake history, [8] proposed a model with three states: a computational cell in state 0 is locked; that is, the cell is not slipping in an earthquake. The transition from state 0 to state 1 occurs, when the stress τ in the cell equals the steady-state friction τ^{ss}. This condition can be expressed in terms of the slip speed $\dot{\delta}^{ss}$ and the corresponding state variable θ^{ss}, i.e. $\theta^{ss} = D_c/\dot{\delta}^{ss}$. From Eq. (1) the steady state friction becomes

$$\begin{aligned} \tau^{ss} &= \sigma \left[\mu_0 + (A - B) \ln \left(\dot{\delta}^{ss}/\dot{\delta}^* \right) \right] \\ &= \sigma \left[\mu_0 + (B - A) \ln \left(\theta^{ss}/\theta^* \right) \right] . \end{aligned} \tag{6}$$

The time Δt that elapses until a cell in with state variable θ changes from state 0 to 1 can be calculated by equating Eq. (6) with remote stressing (Eq. 4):

$$\tau_0 + \dot{\tau}\Delta t = \sigma \left[\mu_0 + (B - A) \ln \left(\theta + \Delta t/\theta^* \right) \right]. \tag{7}$$

This equation can be solved numerically for Δt, e.g. by a Newton scheme. The transition to state 1 marks a breakdown of the cell or the begin of the nucleation towards the earthquake. At transition time, the slip speed is set to $\dot{\delta}_0 = D_c/\theta$ and evolves according to Eq. (5), until a predefined value $\dot{\delta}_{\mathrm{EQ}}$ is reached. The cell changes to state 2, i.e. it slips in an earthquake associated with the redistribution of stress to other cells. When the stress is again below the steady-state stress, the cell changes from state 2 to 0.

The model algorithm can be described as follows. First, we consider a spatial grid, where each cell is represented by an index n. Shear stress, state variable and slip speed are thus denoted by τ_n, θ_n, and $\dot{\delta}_n$. The stress loading rate $\dot{\tau}_n$ is calculated from the static Green's function G_{nm} of the elastic half-space [14]:

$$\dot{\tau}_n = \dot{\delta}_{\mathrm{EQ}} \sum_{m \neq n} G_{nm}. \tag{8}$$

The numbers G_{nm} correspond to the response on a static dislocation of a rectangular fault patch in an elastic Poisson solid with rigidity 30 GPa. Since the Green's function is only calculated within a plane, the diagonal elements have are negative, while the off-diagonal elements have positive sign; that is, if a cell slips, the stress in all other cells increases.

1. Set initial conditions for $\tau_n, \dot{\delta}_n$, and θ_n. All cells are in state 0.
2. Calculate $\Delta t_{n,0\to1}$ from Eq. (7) for all cells. The cell k with the smallest value $\Delta t_{0\to1,\min}$ changes to state 1. Update stress and state variable of remaining cells:

$$\begin{aligned} \tau_n &\to \tau_n + \Delta t_{0\to1,\min} \dot{\tau}_n \\ \theta_n &\to \theta_n + \Delta t_{0\to1,\min} \end{aligned} \tag{9}$$

and set

$$\dot{\delta}_{0,n} = D_c/\theta_n. \tag{10}$$

3. Calculate $\Delta t_{n,0\to1}$ and $\Delta t_{0\to1,min}$ for all cells in state 0, and the time $\Delta t_{n,1\to2}$ of the potential transition of the nucleating cell k from state 1 to state 2

$$\Delta t_{k,1\to2} = \frac{A\sigma}{\dot{\tau}_k} \ln\left(\frac{1}{\dot{\delta}_{k,0}} + \frac{H\sigma}{\dot{\tau}_k}\right) - \frac{A\sigma}{\dot{\tau}_k} \ln\left(\frac{1}{\dot{\delta}_{\mathrm{EQ}}} + \frac{H\sigma}{\dot{\tau}_k}\right) \tag{11}$$

   (a) If $\Delta t_{k,1\to2}$ is smaller than all potential transition times form state 0 to 1, perform transition of cell k from state 1 to 2: Update stress values for *all* cells and state variables θ_n for locked cells:

$$\begin{aligned} \tau_n &\to \tau_n + \Delta t_{k,1\to2}\dot{\tau}_n \\ \theta_n &\to \theta_n + \Delta t_{k,1\to2}. \end{aligned} \tag{12}$$

   According to [8], the stress loading rates are assumed to be constant during a time step and only change when a cell starts (or stops) slip. In particular, if cell k changes to state 2, the stress loading rates for cells $n \neq k$ are increased:

$$\dot{\tau}_n \to \dot{\tau}_n + G_{nk}\dot{\delta}_{\mathrm{EQ}}. \tag{13}$$

   (b) If $\Delta t_{0\to1,\mathrm{min}}$ (related to a cell m) is smaller than $t_{n,1\to2}$, perform step 2 (transition $0 \to 1$) for cell m and proceed.

4. When the stress in a cell with state 2 drops to the steady-state value,

$$\tau_n \leq \tau_n^{ss}, \tag{14}$$

   perform transition from state 2 to 0 for this cell. Update $\tau_n, \dot{\delta}_n$, and θ_n and set stressing rate back according to Eq. (8). Proceed with step 2.

We note that the computational effort is reduced drastically compared to the model version with differential equations, because the elastostatic interaction enters only in state 2, while in states 0 and 1, the cells do not interact with each other. In particular, the stress interaction during the nucleation period is neglected. For further discussion, we refer to [8]

2.1.3 1D model versions

The setup of the 1D model is illustrated in Fig. 1. It is assumed that the extension of the fault towards depth is infinite; this symmetry along depth reduces the model essentially to a one dimensional chain along strike. The question is now: Can a stable solution evolve from $n = -\infty$ to $n = +\infty$ along the chain? If this is possible, we further study whether the framework of RS friction leads to constraints of the rupture velocity. Two implementations of the 1D model are considered: 1. Model A: An infinite half-chain is in state 1 and ruptures cell-by-cell to state 2 (see Fig. 2); 2. Model B: An infinite half chain is in state 0; due to tectonic loading, transitions to state 1 are initiated at the breakdown front. The subsequent rupture evolution is characterized by transitions from state $0 \to 1$ or from state $1 \to 2$ depending on the smallest time-to-failure. After some time, the chain will include a number of slipping cells (state 2), followed by a nucleation zone (state 1) and the remaining cells which are still locked (state 0); see Fig. 3.

2.1.4 Parameters

In this study, we use commonly adopted values for RS friction [8]. All parameters of this study as listed in Tab. 1.

3 Simulations and Results

We now consider the two versions of the 1D model described above with respect to the existence of a stable steady state solution traveling from $-\infty$ to $+\infty$.

3.1 Model A

In the simple model (model A) illustrated in Fig. 2, where only transitions from the nucleating regime (state 1) to the slipping regime take place, the model evolution is governed by Eq. 11: the cell at the front separating nucleating and slipping regime, which is still in state 1, will change to state 2 after the time $\Delta t_{k,1\to 2}$, which depends on the difference of the actual slip rate $\dot{\delta}_{k,0}$ and the imposed earthquake slip rate $\dot{\delta}_{\mathrm{EQ}}$. A steady-state solution is defined by the condition that the spatial distribution of slip speed $\dot{\delta}$ remains the same relative to the rupture front for evolving time, i.e. $\dot{\delta}_{n,t=0} = \dot{\delta}_{n,t=t_1}$ for all times t_1 (see Fig. 2). Here and in the following n denotes the number of cells *relative* to the front. This requires that the map

$$\dot{\delta}_{n+1} = \left\{ \left[\frac{1}{\dot{\delta}_n} + \frac{H\sigma}{\dot{\tau}_{n+1}} \right] \left[\exp\left(\frac{\dot{\tau}_{n+1}\Delta t}{A\sigma} \right) \right] - \frac{H\sigma}{\dot{\tau}_{n+1}} \right\}^{-1} \tag{15}$$

based on the inversion of Eq. (5) has a fix point, i.e. a point $\dot{\delta}^*$ with $\dot{\delta}^*_{n+1} = \dot{\delta}^*_n$. It is found that $\lim_{n\to\infty} \dot{\delta}_n = 0$ for all parameter choices. Consequently, rupture velocity $v_{\mathrm{r}} = \Delta x/\Delta t$ is determined by the time step in Eq. (11); Δx is the width of a cell. In particular, v_{r} depends on the slip speed just before the rupture front and can take values between $v_{\mathrm{r}} = 0$ ($\dot{\delta}_0 = 0$) and $v_{\mathrm{r}} \to \infty$ ($\dot{\delta}_0 \approx \dot{\delta}_{\mathrm{EQ}}$).

Now a (non steady-state) distribution $\dot{\delta}_n$ is imposed and Δt (or $v_{\mathrm{r}} = \Delta x/\Delta t$) is iterated. Assuming a decaying initial distribution

$$\dot{\delta}_n = \dot{\delta}_{n=0} \exp\left(-\beta n \Delta x\right) \tag{16}$$

1. Δt is calculated at the rupture front (Eq. (11)),
2. $\dot{\delta}_n$ is updated (Eq. (15)) and
3. Δt is calculated at the new rupture front etc.

It is found that all initial distributions of $\dot{\delta}_n$ converge to a steady state in terms of a specific value v_{r}. Figure 4 shows an example with $\dot{\delta}_{n=0} = 2 \cdot 10^{-5}$ m/s and two different values for the decay rate β.

In sum, we find that this version of the model obeys stable steady-state solutions for 1D rupture propagation. Clearly, an initial distribution of slip speeds along the chain has to decay with increasing distance from the rupture front in order to allow for a steady state. Again, we find that all rupture velocities are, in principle, possible. A weakly decaying distribution will result in high values of v_{r}; in the limit of a constant distribution, v_r will diverge to ∞. In a rapidly decaying distribution, more time is needed for the cells to reach the earthquake slip speed δ_{EQ} and v_r will thus be smaller.

Finally, we emphasize that in model A the evolution of the stress τ is not yet considered. Implicitly we assume that the stress of cells in state 2 is high enough that a transition from state 2 to state 0 (locked) is not possible and the rupture continues for all times. This, however, requires a constraint for the initial stress τ_0: Because a cell in state 1 does not exchange stress with other cells, the stress increases linearly with time. For this reason, the spatial distribution of stress τ_n requires

$$\tau_n = \tau_{n+1} + \dot{\tau}_{n+1}\Delta t. \tag{17}$$

or

$$\tau_{n+1} = \tau_n - \dot{\tau}_{n+1}\Delta t. \tag{18}$$

The solution of this linear difference equation with initial value τ_0 is given by

$$\begin{aligned}\tau_n &= \tau_0 - \Delta t\dot{\tau}_{n-1} - \Delta t\dot{\tau}_{n-2} - \ldots - \Delta t\dot{\tau}_1 \\ &= \tau_0 - \Delta t \sum_{i=1}^{n-1} \dot{\tau}_i \\ &= \tau_0 - \Delta t\dot{\delta}_{EQ} \sum_{i=1}^{n-1}\sum_{j=0}^{\infty} G_{ij} =: \tau_0 - \tau_a\end{aligned} \tag{19}$$

Choosing $\tau_0 > \tau_{ss} + \tau_a$, the stress τ_n will exceed the steady-state stress τ_{ss} for all times leading thus to an infinite rupture.

3.2 Model B

Model B represents a more realistic framework of earthquake dynamics governed by RS friction than model A, because three different states (locked, nucleating, and slipping) are considered.

Therefore, simulations include the following steps arising from simplification of the model algorithm described in Sec. 2.1.2:

1. Calculation of the potential transition time $t_{1\to2}$ (state 1 $\to$ state 2) before the rupture front as in model A.
2. Calculation of the potential transition time $t_{0\to1}$ using Eq. (7) numerically.
3. If $t_{0\to1} < t_{1\to2}$, perform transition $0 \to 1$, otherwise perform transition $1 \to 2$.
4. Update slip, stress, state variables and stress loading rates and go to 1.

Using uniform distributions of initial stresses $\tau_n(t = 0) \equiv \tau_0$ and initial state variables $\theta_n(t = 0) \equiv \theta_0$, the results indicate that v_r depends mainly on $\dot{\delta}_\mathrm{EQ}$ and τ_0. Transforming $\dot{\delta}_\mathrm{EQ}$ to the dynamic stress drop in a cell where rupture starts, $\Delta\tau$, leads to

$$\Delta\tau = \frac{G}{2v_\mathrm{s}}\dot{\delta}_\mathrm{EQ}, \tag{20}$$

with the shear modulus $G = 30$ GPa and the shear wave velocity $v_\mathrm{s} = 3$ km/s [8]. We consider results of v_r depending on $\Delta\tau$ and τ_0. An example for the evolution of rupture velocity is shown in Fig. 5. Again, the value of v_r approaches a constant value after some time. Figure 6 illustrates the dependence of v_r on $\Delta\tau$ and τ_0. Three regimes with different physical meaning are distinguished by means of the shear wave velocity $v_\mathrm{s} = 3$ km/s and the pressure wave velocity $v_\mathrm{p} = 5.2$ km/s. While the regimes with sub-shear ruptures ($v_\mathrm{r} < v_\mathrm{s}$) and super-shear ruptures ($v_\mathrm{s} < v_\mathrm{r} < v_\mathrm{p}$) resemble physically plausible behavior, a large fraction of the parameter space spanned by $\Delta\tau$ and τ_0 is characterized by $v_\mathrm{r} > v_\mathrm{p}$, that is a non-causal model.

In general, the rupture velocity can become arbitrarily high (for τ_0 close to the steady-state stress τ_ss), there is a lower bound $v_\mathrm{r} \neq 0$ for an unloaded state-0-region ($\tau_0 = 0$). For commonly assumed values of the dynamic stress drop $\Delta\tau = 10$ MPa$\ldots$50 MPa and initial stresses $\tau_0 \leq 0.7\tau_\mathrm{ss}$, the rupture velocity take values $v_\mathrm{r} = 1$ km/s$\ldots$11 km/s.

A main goal of this work is to provide constraints for model parameters leading to realistic model earthquake dynamics. Setting up an earthquake simulator for a specific region, model parameters leading to non-causal model behavior should be excluded. Whether or not sub-shear or super-shear can be considered as realistic, depends on the region under consideration.

4 Conclusions

Earthquake simulators are models for earthquake evolution with reduced physics that allow for the calculation of long earthquake sequences. While traditional seismic hazard calculations are based on the memory-less Poisson process and do not account for clustering in space and time, earthquake simulators are capable to include physical properties to some extent. An important challenge is to find a reasonable balance between realistic earthquake evolution on

the one hand, and simplicity in the sense of low computational effort and only few adjustable parameters on the other hand. RS friction has turned out to be a key ingredient for earthquake physics, because of the experimental evidence (lab scale) and the ability to reproduce observed earthquake clusters in numerical models on the scale of fault systems [7]. The earthquake simulator proposed by [8] and extended by [18] may serve therefore as an attractive tool for modern seismic hazard assessment.

In this study, we have simplified the two-dimensional model to a one-dimensional model obeying symmetry along depth. In order to provide constraints for model parameters, we study the existence of stable steady-state solutions of one-dimensional ruptures with well-defined rupture velocity v_r. The follow-up question is, whether reasonable values of v_r can be attributed to parameters of the model. Two implementations are considered: 1. an infinite half plane, which is already nucleating, breaks down cell-by-cell; 2. the half plane is locked initially and undergoes nucleation and breakdown in series. The latter model is a 1D simplification of the original model of [8].

The results indicate that stable steady-state solutions of a 1D rupture exist in both models. The framework of RS friction alone does not provide constraints for the rupture velocity v_r. The value of v_r mainly depends on the initial state of the system: For a near-to-critical state, v_r can be arbitrarily high, while the value will be small, if the system is far from criticality at the begin of the simulation. In the more realistic model, v_r also depends on the earthquake slip speed, or the corresponding value of the local stress drop. Imposing reasonable values for the velocities of the seismic waves, v_s and v_p, it becomes possible to distinguish regimes in parameter space that are characterized by sub-shear, super-shear, and non-causal rupture propagation. These findings will have impact for the adjustment of the earthquake simulator to a specific fault zone.

Future research in this direction includes both, theoretical and practical aspects. With respect to the fix point in model A, it is interesting to conduct a more detailed analysis of the stability of the fix point. So far, we have demonstrated that each spatially decaying distribution of slip speeds leads to the convergence of v_r. However, if the distribution is disturbed, it has to be investigated, whether v_r converges to the same value or to a different value. Regarding the practical research, we have focused on a small part of the parameter space. Further constraints, e.g. for parameters related to RS friction, have to be employed.

Acknowledgments

This work was supported by the "Deutsche Forschungsgemeinschaft" (SFB 555 and HA4789/2-1) and the Potsdam Research Cluster for Georisk Analysis, Environmental Change and Sustainability (PROGRESS). We are also grateful to an anonymous reviewer for comments that helped to improve the manuscript.

References

1. Bak, P., Tang, C., Geophys. Res. Lett., **94**, (1989), 15635-15637
2. Ben-Zion, Y., J. Mech. Phys. Solids, **49**, (2001), 2209-2244
3. Ben-Zion, Y., Rice, J. R., J. Geophys. Res. **98**, (1993) 14109-14131
4. Brietzke, G., Cochard, A., Igel, H., Geophys. Res. Lett., **34**, (2007), L11305, doi:10.1029/2007GL029908
5. Dieterich, J. H., *Mechanical Behavior of Crustal Rocks, Geophys. Monogr. Ser.* (AGU, Washington, D.C., 1981) 103-120
6. Dieterich, J. H., Tectonophys. **211**, (1992) 115-134
7. Dieterich, J. H., J. Geophys. Res. **99**, (1994) 2601-2618
8. Dieterich, J. H., Nonlin. Proc. Geophys. **2**, (1995) 109-120
9. Dieterich, J. H., Treatise in Geophysics **4**, (2007) 107-129
10. Gutenberg, B., Richter, C., Bull. Seism. Soc. Am. **46**, (1956) 105-145
11. Hainzl, S., Zöller, G., Wang, R., J. Geophys. Res. **115**, (2010), doi: 10.1029/2008JB006224

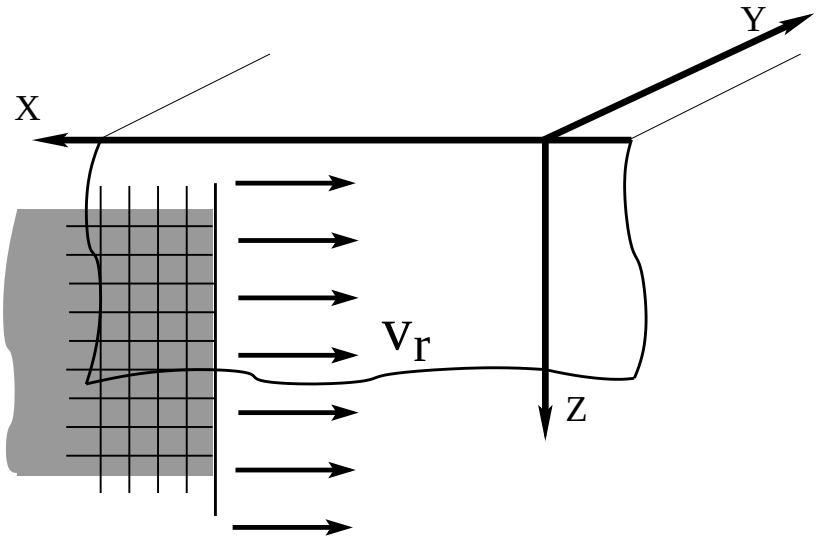

Fig. 1. Sketch of the fault model.

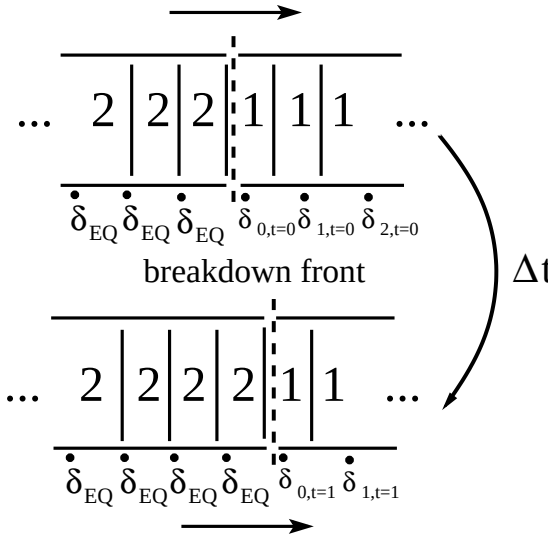

Fig. 2. Model A: 1D Rupture evolution from state 1 (nucleating) to state 2 (earthquake).

12. Matthews, M., Ellsworth, W., Reasenberg, P., Bull. Seism. Soc. Am. **92**, (2002), 2233-2250
13. Ogata, Y., J. Am. Stat. Assoc., **83**, (1988) 9-27
14. Okada, Y., Bull. Seism. Soc. Am. **82**, (1992), 1018-1040
15. Omori, F., J. Coll. Sci. Imp. Univ. Tokyo (1894), 111-200
16. Ruina, A. L., J. Geophys. Res. **88**, (1983) 10359-10370
17. Rundle, P. B., Rundle, J. B., Tiampo, K. F., Donnellan, A., Turcotte, D. L., Pure Appl. Geophys. **163**, (2007), 1819-1846
18. Smith, D. E., Dieterich, J. H., Pure Appl. Geophys. (2010) doi: 10.1007/s00024-010-0093-1
19. Vere-Jones, D, J. Phys. Earth **26**, (1978), 129-146
20. Zöller, G., Hainzl, S., Holschneider, M., Bull. Seism. Soc. Am. **98**, (2008), 2641-2651
21. Zöller, G., Holschneider, M., Ben-Zion, Y., Pure Appl. Geophys. **161**, (2004), 2103-2118

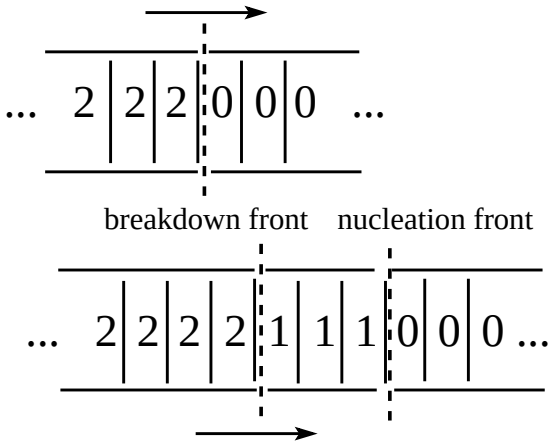

Fig. 3. Model B: 1D Rupture evolution from state 0 (locked) via state 1 (nucleating) to state 2 (earthquake).

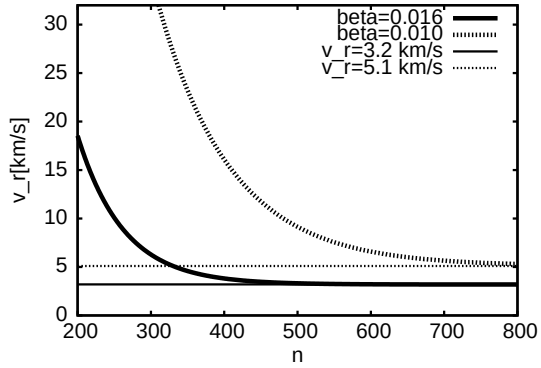

Fig. 4. Evolution of v_r for two different initial distributions of slip speeds $\dot{\delta}_n$.

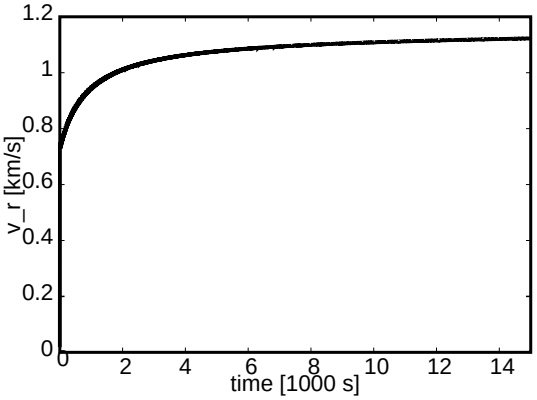

Fig. 5. Model B: Rupture velocity v_r as a function of time for $\tau_0/\tau_\mathrm{ss} = 0.5$ and $\Delta\tau = 5$ MPa.

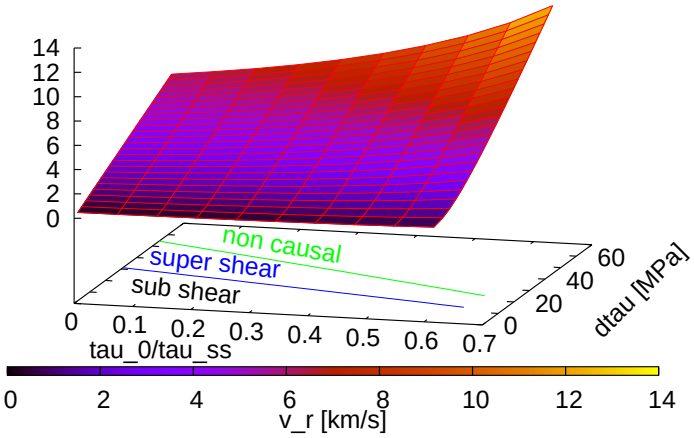

Fig. 6. Model B: Transition from sub to super shear rupture (based on $v_s = 3$ km/s) is indicated as a blue contour line, the transition to non causal behavior ($v_r > v_p$ with $v_p = 5.2$ km/s) is marked as a green contour line.

Table 1. Model parameters.

parameter	value
normal stress σ	15 MPa
friction coefficient μ_0	0.6
A	0.005
B	0.015
D_c	10^{-5} m
θ^*	1 s
cell size Δx	1 km
shear modulus G	30 GPa
earthquake slip speed $\dot{\delta}_{EQ}$ (in model A)	1 m/s
v_s	3 km/s
v_p	5.2 km/s